

# Computer Methods and Programs in Biomedicine

## A Systematic Comparison Between FEBio and PolyFEM for Biomechanical Systems

--Manuscript Draft--

<b>Manuscript Number:</b>	CMPB-D-23-01223
<b>Article Type:</b>	Full Length Article
<b>Section/Category:</b>	Modelling & Simulation
<b>Keywords:</b>	Finite element analysis, Large deformation, Contact, Benchmark, Finite element verification
<b>Corresponding Author:</b>	Teseo Schneider University of Victoria Victoria, BC CANADA
<b>First Author:</b>	Liam Martin
<b>Order of Authors:</b>	Liam Martin  Pranav Jain  Zachary Ferguson  Torkan Gholamalizadeh  Faezeh Moshfeghifar  Kenny Erleben  Daniele Panozzo  Steven Abramowitch  Teseo Schneider
<b>Manuscript Region of Origin:</b>	North America
<b>Abstract:</b>	<p>Simulations of biomechanical systems are fundamental to studying pathological processes; they are particularly challenging as they often contain thin, soft layers, complex collisions scenario, and large deformations. Most existing simulators are not robust in handling these common scenarios.</p> <p>In this paper, we evaluate the applicability of a novel approach, implemented in the open-source package PolyFEM, to a benchmark of problems in biomechanics to understand their potential. While the technology is new, and many features are still missing -- we highlight which ones are more important for biomechanics to guide future development. We show that PolyFEM, which includes high-order simulation within the incremental potential framework, is well-suited for many biomechanical applications. Accuracy and runtime are comparable to FEBio, but PolyFEM is more robust and can handle complex collision and compression cases not supported by other approaches.</p>
<b>Suggested Reviewers:</b>	Jeffery Weiss The University of Utah jeff.weiss@utah.edu John Rasmussen Aalborg University jr@mp.aau.dk Marie Traberg Technical University of Denmark msene@dtu.dk
<b>Opposed Reviewers:</b>	

Dear Editor,

We submit our manuscript entitled “A Systematic Comparison Between FEBio and PolyFEM for Biomechanical Systems” to your consideration for publication in the Computer Methods and Programs in Biomedicine.

We believe that the work, which contains a large evaluation of biomechanical simulation for FEBio and PolyFEM, will be of high interests to the readers of the journal. It provides new insights that we believe will expose biomechanical practitioner to novel robust FE solvers.

We commit on publicly releasing the experimental description, meshes, and reference implementation of our testing infrastructure in the additional material.

Sincerely,  
The Authors

## Highlights

### **A Systematic Comparison Between FEBio and PolyFEM for Biomechanical Systems**

- Large benchmark for biomechanical system.
- PolyFEM is comparable to FEBio in term of results and performance, but is much more robust for large deformations and contacts.
- PolyFEM lacks some features (e.g., intuitive UI, shell modelling, rigid bodies).

## Highlights

### A Systematic Comparison Between FEBio and PolyFEM for Biomechanical Systems

Liam Martin, Pranav Jain, Zachary Ferguson, Torkan Gholamalizadeh, Faezeh Moshfeghifar, Kenny Erleben, Daniele Panozzo, Steven Abramowitch, Teseo Schneider

- Large benchmark for biomechanical system.
- PolyFEM is comparable to FEBio in term of results and performance, but is much more robust for large deformations and contacts.
- PolyFEM lacks some features (e.g., intuitive UI, shell modelling, rigid bodies).

# A Systematic Comparison Between FEBio and PolyFEM for Biomechanical Systems

Liam Martin<sup>a</sup>, Pranav Jain<sup>b</sup>, Zachary Ferguson<sup>b</sup>, Torkan Gholamalizadeh<sup>c</sup>, Faezeh Moshfeghifar<sup>d</sup>, Kenny Erleben<sup>d</sup>, Daniele Panozzo<sup>b</sup>, Steven Abramowitch<sup>a</sup> and Teseo Schneider<sup>e,\*</sup>

<sup>a</sup>*University of Pittsburgh Swanson School of Engineering, USA*

<sup>b</sup>*New York University, USA*

<sup>c</sup>*3Shape A/S, Denmark*

<sup>d</sup>*University of Copenhagen, Denmark*

<sup>e</sup>*University of Victoria, Canada*

## ARTICLE INFO

### Keywords:

Finite element analysis  
Large deformation  
Contact  
Benchmark  
Finite element verification

## ABSTRACT

Simulations of biomechanical systems are fundamental to studying pathological processes; they are particularly challenging as they often contain thin, soft layers, complex collisions scenario, and large deformations. Most existing simulators are not robust in handling these common scenarios.

In this paper, we evaluate the applicability of a novel approach, implemented in the open-source package PolyFEM, to a benchmark of problems in biomechanics to understand their potential. While the technology is new, and many features are still missing – we highlight which ones are more important for biomechanics to guide future development. We show that PolyFEM, which includes high-order simulation within the incremental potential framework, is well-suited for many biomechanical applications. Accuracy and runtime are comparable to FEBio, but PolyFEM is more robust and can handle complex collision and compression cases not supported by other approaches.

## 1. Introduction

Simulations of biomechanical systems are often used as a controlled and cost-effective way to make predictions of normal and/or pathological processes, to gain insights into these complex systems through parametric analyses, to design devices, as an indirect and non-invasive way to perform measurements, and as a way to communicate and educate [60, 22, 30, 2, 47, 54, 10]. Traditionally, computational biomechanics, and bioengineering in general, have benefited significantly from adapting theories and approaches developed to solve traditional engineering problems with traditional materials. For example, rubber elasticity provided an excellent general framework for understanding the fundamentals of tissue mechanics. However, many of these tools were never designed specifically to solve problems in biomechanics so they often fail to sufficiently describe specific aspects of biological mechanical behavior that are often required to answer specific biological questions (e.g. rubber elasticity cannot describe tissue growth and remodeling) [29].

Energy transfer via contact and friction is particularly challenging for simulations and proves to be especially problematic in the context of biological tissues. Compared to standard engineering materials, biological tissues can undergo very large non-linear deformations, even in response to relatively small forces, and are often in contact with other tissues that are mutually deformable. Small errors in the calculation of forces can result in very large deformations that do not accurately simulate the system. Thus, it is not only important to accurately describe material behaviors

in these scenarios, it is also critical to accurately describe mechanical interactions between materials that share contact surfaces.

For most scenarios, there are a few common configurations that are particularly challenging:

1. thin, soft layers compressed between large and stiff objects (for example, cartilage and menisci),
2. high-energy collisions,
3. large deformations of soft tissues,
4. complex contact between multiple objects in close proximity.

In all these cases, there are often failures due to either individual elements degenerating into zero or negative volume (often referred to as negative Jacobian elements) or an inability to correctly resolve collisions leading to either invalid simulation states or non-physical impulse forces to compensate for the incorrect collision response. These problems are tackled in existing simulators by providing parameters that allow controlling both contact and elastic forces to prevent these configurations. However, finding a valid set of parameters for scenes with complex geometries and scenarios can be extremely challenging and time-consuming. Furthermore, there is no guarantee that a set of parameters even exists. This can lead to an infinite loop of adjusting parameters that may ultimately never produce a viable result. Once this happens the user either has to make compromises (e.g. changes to the geometries, altering the boundary conditions, or otherwise simplifying the simulation) in order for the simulation to complete.

\*Corresponding author  
ORCID(s):

A new family of robust FE solvers based on the incremental potential contact formulation [35] has been recently introduced for structural mechanics problems: the key difference in these approaches is that their formulation is, by construction, addressing the two issues above. No element can invert and no collision can be missed. This is achieved with an entirely different (and not equivalent) formulation, which trades off computational efficiency for increased robustness and reduction of parameter tuning. In this work, we benchmark the implementation of this approach in the PolyFEM [52] open-source software to evaluate its utility for biomechanical simulations, comparing it against the established FEBio software [38].

We observe that the results obtained by PolyFEM are very similar to FEBio, while requiring much less parameter tuning; in some complex cases, we found that PolyFEM was able to simulate systems that proved too be challenging for FEBio. On the other hand, PolyFEM is still in the early stages of development and thus does not yet support a wide selection of feature that are necessary for many biomechanical simulations, including reduced models of rods and shells, advanced material models, and certain constraints. As noted, it is important to recognize that the ability to handle more complex simulations also comes at a higher computation price; based on our experience, we believe this is a fair tradeoff, as computational resources are affordable compared to the human effort required for parameter tuning.

We believe IPC-based solvers are an ideal fit for biomechanical simulation, despite their current restricted scope, and our work provides guidelines and benchmarks to support the development and research of these techniques for biomechanical purposes. We are excited by the prospect of having the IPC-based solvers in biomechanics, as we believe they could lead to a massive reduction in human effort, and open the door to a larger use of simulation for designing and understanding biomechanical systems.

## 2. Related

### 2.1. Biomechanics Simulations

We note that the list of FE studies and software included in this section is by no means exhaustive. Providing such an exhaustive review is beyond the scope of this work; however, we believe that it is important the contextualize our work by providing a representative selection of other software that is often used in biomechanics research.

A common application for the use of specialized simulation is in the area of musculoskeletal modeling. Software for these simulations is based on using rigid multi-body systems for bones and Hill-based (spring-like) models for muscles [53, 12]. While very important and successful for many questions related to joint kinematics and dynamics, muscle force estimation, and muscle activation patterns, such simulators ignore inter-contact between muscles and model muscle-bone interaction directly via points. The type of problems addressed often implies inverse dynamics and contact with the environment are prescribed as boundary

constraints. Hence, they often do not include the elasticity of tissue and use idealized assumptions on joints and contact, sometimes driven by real-life force measurements. It is not uncommon to use simulation outputs from such simulators to estimate forces that can drive motions in finite-element simulations.

For fast solvers for real-time medical simulations, there exist frameworks such as SOFA [19] which are well designed to provide solutions for pre-guided image surgery, control of soft medical robots, surgical training, and more. SOFA focuses on performance to deliver fast real-time interaction with clinical operators [65]. By using the finite element method with a focus on linear elements and co-rotational linear elastic materials mixed with optimizations of matrix computations that exploit zero-fill patterns, this software can achieve significant performance gains at the cost of accuracy. In terms of contact, the SOFA does support general collision detection and implements constraint-based contact forces using expressed LCP models based on the classic Coulomb friction models for planar dry friction. Nevertheless, these compromises in accuracy in favor of performance are often justified for some problems in biomechanics. SOFA can also be extended. For example, the inverse finite element method is being used in SOFA to support control of soft medical robots [40]. In addition, FEniCSx and SOFA have also been combined [39] providing SOFA with advanced FE features and support for users to implement their constitutive model of choice through coding both for direct forward and inverse simulations.

On the other hand, many problems in biomechanics often necessitate accuracy on a level that cannot be provided by fast real-time medical simulators. These simulations are usually performed using commercial finite element (FE) software packages (e.g., Ansys<sup>TM</sup> [13, 46, 49], ABAQUS<sup>TM</sup> [32, 27, 69, 37], COMSOL [24, 25], and NIKE3D<sup>TM</sup>) or open-source solvers like FEBio (University of Utah) [38, 21, 51, 34] or aforementioned FEniCSx [36]. These solvers have largely evolved from traditional structurally focused engineering solvers, and while they do provide state-of-the-art material models for biomechanics and are often robust to handle many biomechanical scenarios, they were not specifically designed to capture some of the complex mechanical interactions that are common in biomechanics (e.g., large deformation, sudden contact, and friction forces). As such, the contact models are generally most suitable for structural mechanics applications. While these can be effective for specific biomechanical applications (e.g., orthopedics), they often require a large degree of parameter tuning and often explicit specification of the contact surfaces. This can present significant challenges for simulating soft tissue-to-soft tissue interactions with nonuniform geometries that undergo major changes in shape, size, and areas of contact. Even for well-poised problems, incorrect parameter choices can often lead to simulation failure or inaccurate results. Other solvers, such as the SIMon Finite Element Head Model (developed in part by the National Highway Traffic Safety Administration), are designed to simulate specific scenarios; namely head

trauma in motor vehicle accidents [57, 58]. Other studies either used less popular software [56, 50, 14] or did not explicitly state which FE solver they used [18, 66].

## 2.2. Existing Benchmarks of Finite Element Solvers

We are not aware of a comprehensive set of benchmarks that can evaluate an FE solver's ability to compute complex biomechanical problems. Therefore, the responsibility falls on the software developers and model creators to ensure the accuracy of their work. FE benchmarks can be broadly divided into two categories, verification and validation. The former focuses on confirming that the solver produces accurate mathematical solutions, while the latter involves ensuring that the computational model accurately simulates real-world physical interactions [3, 26].

In the past, verification has primarily been the responsibility of the solver's creators, who have released verification problems along with their FE solver. These problems serve to demonstrate that the underlying mathematical implementation is sound by comparing the solver's solutions to known analytical solutions and/or previously verified FE solvers [1, 4, 38]. Although some groups have attempted to compile a comprehensive list of verification problems that should accompany any FE solver, these lists have yet to gain significant adaptation [45, 15, 42, 16]. The most common verification problems are simple simulations with well-known analytical solutions and will be presented in more detail later in the paper (i.e., a cantilever beam, hyperelastic sheet with hole, single element tension/compression, etc.).

Validation, on the other hand, is usually produced to accompany the release of a FE model. In these benchmarks, the model's creator should attempt to prove that their model is capable of modeling real-world physical interactions. In biomechanics, this typically involves one or more of the following: comparing the measures generated by an FE model to experimental biomechanical data, such as stress, strain, and displacement [13, 57, 58, 67, 46, 20, 14, 56, 69, 49], cadaveric and/or human system measures [57, 67, 20, 32, 46, 21, 51, 34], or even other FE solvers [32, 18, 49]. In cases where simple outcome measures are nearly impossible to measure (i.e., *in vivo* tissue response), comparing the motion of organs/tissues on dynamic MRI to that calculated from the model has been used as proxy [50, 37].

Beyond comparing the accuracy of FE solutions, benchmarks offer the ability to compare the efficiency of FE software while simulating the mechanical problem. The easiest of these comparisons to make is the CPU time that it takes for the solvers to converge to the same solution. This notably does not include the time that it takes for the user to set up the simulation, or "human time," which in most cases is the most time-consuming portion of FE model development. Human time also extends to the iterative process where the user has to adjust model parameters (meshes, contact penalties, etc.) in order for the model to converge to a solution. There are not many studies that aim to determine which FE software is the fastest. Those that do compare

solvers are comparing specific components of the software like the contact algorithm or solving method [41, 33]. One of the potential reasons for this lack of study is that the majority of researchers in this field will choose the FE software that they are most comfortable with, even if there are potentially significant time delays in doing so.

## 2.3. Common Contact Models in Biomechanics

Biomechanical simulations often require the accurate modeling of physical interactions (i.e. contact) between different tissues, such as those that occur in joints, organ systems, foot/ground interactions, and others. Detecting and implementing methods to resolve the transfer of energy during these interactions are some of the most challenging areas in biomechanical simulation. In general, three classes of contact have been used to detect and implement contact; node-on-node, node-on-segment, and segment-on-segment [64]. Node-on-node contact can only be used in linear cases with symmetrical meshes and thus will not be discussed further. Node-on-segment contact was first developed to address a common problem in all contact methods, i.e. penetration between the two objects that have entered contact with each other. This is handled by first checking for, and if needed, addressing, intersecting faces [64, 48, 59, 28, 55, 63]. Addressing these intersections is depended on the solver that is used and will be discussed later. A single pass node-on-segment approaches only require that the nodes from one object (object A) do not intersect with the faces of another object (object B), also known as "primary and secondary" surfaces [48]. Two-pass approaches do the same thing as single-pass but also ensure that the nodes from B also do not intersect the faces from A [48]. However, these methods are prone to four major drawbacks, which are discussed in much further detail in Puso et. al. and Erleben [48, 17]:

1. Locking or over-constraint of some nodes
2. Non-smooth contact that leads to jumps in contact forces when nodes from an object slide between the faces of the other
3. The discrete constraints cause jumps when nodes from one object slide off the boundary of the other
4. Inequality equations determine active and inactive constraints

These four drawbacks were the significant driving force behind the development of surface-on-surface algorithms which can address the top three drawbacks [48]. By using the surfaces to calculate contact these algorithms avoid the possibility of nodes getting "locked" in place or experiencing significant jumps due to sliding between surfaces or off of the boundary of the surface. Most software allows the user to select which of these contact detection formulations they want to use. Then the method for enforcing the detected contact is software dependent. Several algorithms have been developed for enforcing contact, and two widely used methods are the penalty and Lagrange multiplier methods [8, 44]. In general, both methods apply a multiplier

that penalizes infeasible solutions, i.e., intersection detected between two objects. The augmented Lagrangian method is a combination of these two methods and is implemented in popular software packages such as FEBio, ANSYS, and ABAQUS [62]. These methods are easier to implement than others we will discuss because they only add a multiplier to the objective function [7]. However, their simplicity can introduce significant bias to the simulation since the choice of penalty is often arbitrary and can significantly impact the outcome [6]. Although these methods work well in simple contact cases, they often struggle when computing high-energy contact between soft deformable bodies, such as human organs.

Other, less popular biomechanical FE software, derive their regularized contact model from Nitsche's method. One such software is CutFEM [9, 11]. CutFEM has been designed to make the problem's discretization as independent as possible from the geometric description and to minimize the complexity of mesh generation while maintaining the accuracy of the FE method [9]. Contact interfaces between two meshes are represented by a level set function that is placed on a background grid of the simulation, which allows for low-quality and/or complex geometries to be modeled without the need for computationally expensive remeshing. By using this discretization method, it becomes much easier to implement Nitsche's method for contact [11]. Nitsche's method and its derived regularized contact models apply a penalty term to the weak form of the governing equations and can be viewed as a generalization of the classic penalty model. However, unlike the classical penalty model, Nitsche's method is symmetric and consistent across boundaries, which works well with CutFEM's implementation of geometric boundaries. Symmetry across boundaries ensures that these methods do not suffer from any of the aforementioned locking or jumping effects. Unfortunately, in nonlinear cases, Nitsche's method becomes more complex than penalty or Lagrange methods and thus more challenging to compute. This becomes problematic in biomechanical simulations as the majority of them include some sort of nonlinear contact [63]. Additionally, Nitsche's method uses a penalty parameter that must be arbitrarily assigned and has a significant effect on the simulation outcome. The final type of contact models to be discussed are those based on barrier stiffness methods. These methods are utilized in PolyFEM, which employs the IPC contact library [35]. A barrier stiffness model operates by introducing a stiffness term that prohibits two contacting bodies from intersecting. At the time of their publication Li et al. stated that IPC is the first implementation of a contact model that can ensure convergence of solutions free of intersections and inversions (which, based on another literature search, appears to remain true) [35]. This makes barrier stiffness methods particularly suitable for problems with significant nonlinear deformations, such as those encountered in biomechanical simulations. However, it should be noted that the suitability of this software for biomechanical simulations has not yet

been verified, which is something we will aim to assess in subsequent sections.

### 3. Preliminaries

We briefly overview the major solver differences between FEBio and PolyFEM, focusing on their relevance in biomechanics. We exclude from our discussion friction forces; we refer an interested reader to Maas et al. [38] and Li et al. [35] for more details. The major difference between the two solvers is that PolyFEM expresses all parts (elasticity, inertia, contact, etc.) as potentials, while FEBio uses only the elastic energy. While both formulations are mathematically equivalent, the PolyFEM formulation allows using a standard Newton method coupled with a line search to ensure that the solution remains in the feasible region, thereby having the capability of handling challenging cases such as small elements being compressed or high velocities leading to large deformations. Granted this will lead to a harder minimization problem that might require more iterations for the quadratic approximations of the Newton solver; however, the method is inherently robust as it is guaranteed to produce a physically valid configuration for any provided displacement or velocity (i.e., the solver remains in the feasible region).

*Elastic Potential.* Both FEBio and PolyFEM use the same elastic potential  $E_e$  derived from the elastic energy. However, FEBio supports more material models; for instance, transversely isotropic (Transversely Isotropic Hyperelastic) and orthotropic (Fung Orthotropic, Holzapfel-Gasser-Ogen) materials are not yet implemented in PolyFEM. The major advantage of the potential formulation in PolyFEM is that in the line search, it explicitly checks for inverted elements and shortens the Newton increment to ensure that the new solution is valid. This occurs since the quadratic approximation of  $E_e$  used by the solver does not diverge when elements have zero volume, even if  $E_e$  does. We show an example of such a problem in Figure 2. While this may seem like a minor change, it is possible to implement it only because of the difference in how the solver is set up.

*Inertia Potential.* FEBio implements the standard time integration scheme<sup>1</sup> while PolyFEM uses the incremental potential formulation [31]. Both formulations are equivalent and support several standard time integrators (e.g., Newmark or backward differentiation formula). In PolyFEM, the inertia potential is simply summed to the elastic potential.

*Contact Potential.* While the previous potentials (elastic and inertia) are identical, PolyFEM and FEBio handle contact differently. From a high-level, point of contact requires a set of nodal positions  $x^t$  and nodal velocities  $v^t$ , a choice of spatial and temporal discretization, and a measure of overlap between primitives  $g(x)$ , and obtains the updated nodal positions by solving a constrained minimization of

<sup>1</sup><https://help.febio.org/docs/FEBioTheory-4-0/TM40-Chapter-6.html>

a potential  $E$  [31] (inertia and elasticity in PolyFEM and elasticity in FEBio):

$$x^{t+1} = \operatorname{argmin}_x E(x, x^t, v^t), \quad \text{s.t. } g(x) \geq 0. \quad (1)$$

The choice of  $g$  varies, but it is usually a function that is zero when elements do not overlap and negative otherwise. There are many ways of defining; for instance, FEBio uses the signed distance along the normal direction between the closest points [68]. This problem is typically solved using off-the-shelf or custom numerical solvers; FEBio uses a Newton-Raphson method [38]. As for the elastic potential  $E_e$ , the solution of (1) with linearized constraints does not directly imply that  $g(x) \geq 0$ , and even solving a sequence of problems with linearized constraints at each step might not necessarily find a valid configuration satisfying the non-linear constraints, thus potentially not resolving collisions. We show an example of such failure in Figure 8. Another source of failure is that constrained solvers usually only satisfy the constraints up to numerical precision. This might lead to missed/problematic collisions when large or small numbers are present (e.g., in the presence of high velocities or small elements).

*Incremental potential contact.* The IPC formulation tackles these failure points by avoiding the use of constrained solvers and making the linearization of constraints and energy safe by using a custom line search procedure, as for  $E_e$ . The constrained optimization problem (1) is converted into the unconstrained optimization of:

$$B_t(x) = E(x, x^t, v^t) + \kappa \sum_{k \in C} b(d_k(x)),$$

where  $\kappa > 0$  is an adaptive parameter controlling the barrier stiffness,  $d_k$  measures the distance between two primitives in the set of all possible primitive pairs  $C$ , and  $b$  is a logarithmic barrier function. This non-linear energy is minimized with a Newton descent algorithm with a custom line search that explicitly prevents crossing configurations where  $B_t(x)$  is infinite; that is when two primitives are at zero distance (i.e., there is an overlap between two primitives). These two conditions are tested with algorithms that are exact under floating point rounding [61].

## 4. Methods and Results

We compared each of the solvers in four head-to-head comparison tests. We selected the first two benchmarks, *FEBio-Test* (Section 4.1) and *FEBio-Verification* (Section 4.2), to validate the capability of PolyFEM to conduct simulations similar to those previously published by FEBio [5, 38]. We designed the third benchmark, *Planet-Fall* (Section 4.3) to introduce a high degree of non-linearity into the simulation and to emphasize PolyFEM’s potential as a FE software in complex biomechanics simulations. Finally, the fourth benchmark, *Hip-and-Jaw* (Section 4.4), serves as a real-world example, using patient data, of using PolyFEM as a biomechanics solver [43, 23].

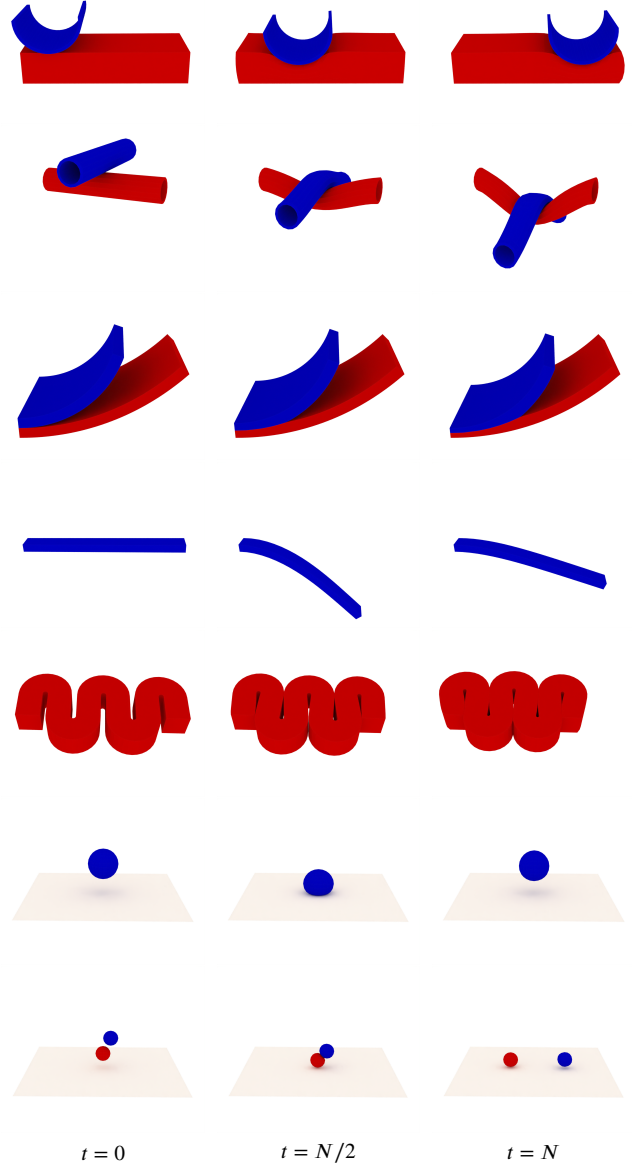


**Figure 1:** Results of 7 dynamic simulations from the FEBio-Test dataset. Each row corresponds to one example simulated from  $t = 0$  to  $t = N$ .

### 4.1. FEBio Test Suite Examples

The test suite is a set of examples that outline the features of FEBio, including static, dynamic, and contact simulations. We selected a group of 18 problems from the test suite, while also adding a new one, and simulated them all using both solvers. Of the 18 selected simulations, 9 are static and involve contact, while the other 9 are dynamic (Figure 1 shows three frames for 7 examples). We ran our simulations on AMD Ryzen Threadripper PRO 3995WX, 64 Core (2.7GHz) sWRX8 Processor, 2TB 3200 MHz DDR4 memory, Ubuntu 22.04.1 LTS using a maximum of 16 threads. Depending on the simulation, outputs for comparisons included displacement or stress, and simulation time in terms of performance. Both FEBio and PolyFEM

**Table 1**

Timings for the simulations from FEBio-Test dataset.

Simulation	Category	PolyFEM (s)	FEBio (s)
co07	Static	13.237	12.1
co16	Static	4.122	0.047
co20	Static	66.811	52.169
co21	Static	15.550	52.764
co32	Static	0.280	0.136
co34	Static	30.114	0.412
co35	Static	91.887	0.095
co41	Static	57.223	5.794
co44	Static	4.371	0.058
dy01	Dynamic	0.330	0.015
dy02	Dynamic	10.663	0.259
dy03	Dynamic	29.567	23.596
dy04	Dynamic	38.474	5.667
dy07	Dynamic	2.918	0.126
dy09	Dynamic	181.853	332.919
dy10	Dynamic	0.176	0.023
dy11	Dynamic	0.477	0.024
dy12	Dynamic	1.407	0.031

produce similar results; but PolyFEM, in general, takes more time to simulate. Table 1 lists the time taken by PolyFEM and FEBio on the selected simulations. We note that the FEBio TestSuite was carefully tuned to work best for FEBio while the PolyFEM simulations were simply automatically converted and worked without any manual tuning.

To highlight the differences in the solver's performance when modeling deformation of very soft elastic materials, we created a new simulation using geometry from the existing benchmark, dyn02, a  $20\text{ m} \times 2\text{ m} \times 1\text{ m}$  rectangular block in a beam bending scenario. The simulation was first changed to be a static simulation. The beam was oriented parallel to the world's x-axis. We modeled the material as Neo-hookean with  $E = 100\text{ Pa}$ ,  $\nu = 0.0$ , and  $\rho = 1$ ) and meshed it within FEBio using tetrahedral elements ( $N_x = 20$ ,  $N_y = 10$ ,  $N_z = 4$ ,  $X - bias = 1.4$ ,  $Y - bias = 1$ ,  $Z - bias = 1$ ). We fixed the left side along all three axes (negative x direction) and limited the front side from deflecting into/out of the page (positive z direction). On the right side of the block (positive x direction), we prescribe a vertical displacement (in the positive y direction) until FEBio failed using the default simulation settings, which occurred at 21 m of vertical deflection. We then replicated the same simulation in PolyFEM but prescribed a vertical deflection of 22 m (one meter more than what FEBio was able to handle). It is important to note that both solvers produced the same solution for 21 m of vertical deflection, which is shown in Figure 2. Although this is an extreme example designed to produce a failed solution in FEBio, it highlights PolyFEM's ability to handle large hyperelastic deformations without inverting elements.

## 4.2. FEBio Verification Examples

Our second set of comparisons was based on the verification paper released by FEBio, which compares the results of FEBio to analytical results, as well as results generated with ABAQUS™ and NIKE3D™ [38]. The paper outlines ten

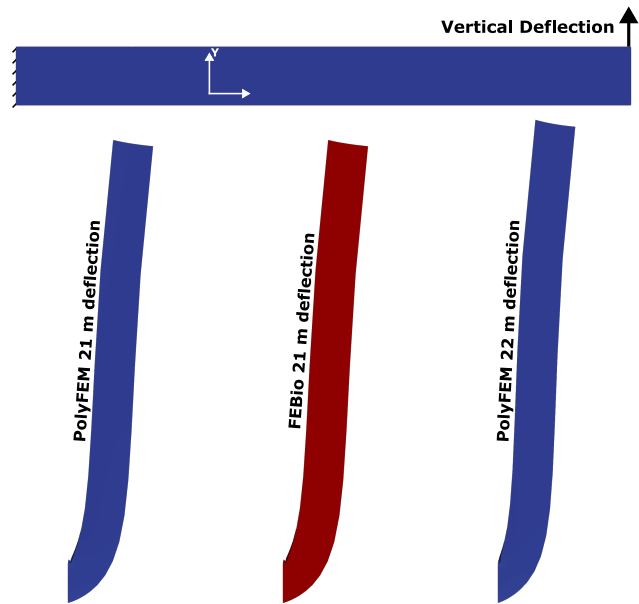


**Figure 2:** A  $20\text{ m} \times 2\text{ m} \times 1\text{ m}$  rectangular block deflected in the y direction from the right-hand side. The first figure shows the setup in its undeformed configuration, and the second and third image shows the FEBio and PolyFEM results, respectively, for a deflection of 21 m. The final picture shows the results for a deflection 22 m using PolyFEM, as FEBio cannot find a solution.

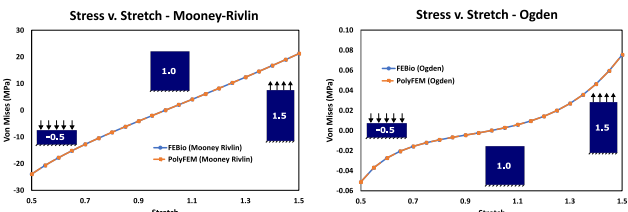


**Figure 3:** Comparison of the von Mises stress versus stretch between PolyFEM and FEBio for a single hexahedral element modeled with two material models.

simulations and verified the results from FEBio with respect to the other two solvers. Thus, the following section not only serves to verify the results from PolyFEM with FEBio but also the other two solvers by extension. All simulations were conducted using PolyFEM and FEBio using the same computer by the same author (2017 iMac Pro, 10 Core (3GHz) Intel Xeon W, 128 Gb 2666 MHz DDR4 memory, macOS Ventura 13.0.1).

The initial example uses a single hexahedral element mesh and compresses it to 0.5 times and stretches it to 1.5 times its original length in one axis. As the dimensions of the geometry were not specified by [38], we choose a  $1\text{ mm} \times 1\text{ mm} \times 1\text{ mm}$  cube. We evaluated the resulting stress inside the element using two different material models, namely the Mooney-Rivlin ( $C_1 = 6.8\text{ MPa}$ ,  $C_2 = 0$ ,  $K = 100\text{ GPa}$ ) and the Ogden hyperelastic ( $N = 1$ ,  $c_1 = 0.0329\text{ MPa}$ ,  $m_1 = 6.82$ ). We plot the von Mises stress (for

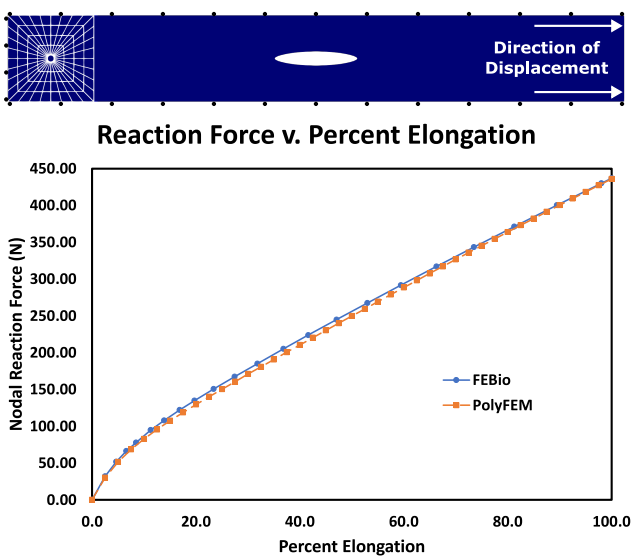
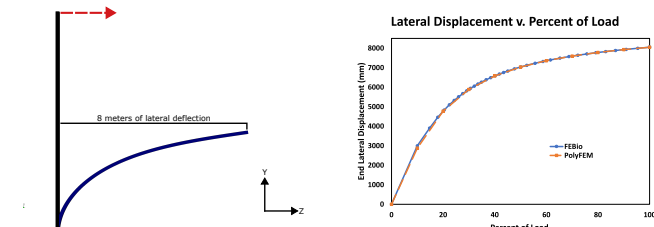


**Figure 4:** Hyperelastic sheet stretched to 615% of its initial length. The top frame shows the sheet (blue) and rollers (black). At the bottom, we plot the reaction forces from the left side of the sheet.

both material models) to compare the results between FEBio and PolyFEM (Figure 3); both solvers produce the same values in tension and compression.

The next example modeled a hyperelastic sheet placed under extreme deformations. The sheet's undeformed dimensions are 165 mm  $\times$  165 mm  $\times$  2 mm with a circular hole ( $r = 6.35$  mm) cut in the center of the large face (Figure 4 top). We meshed it with 128 hexahedral elements and modeled the material as Mooney-Rivlin ( $C_1 = 0.1863$  MPa,  $C_2 = 0.00979$  MPa,  $K = 100$  MPa). The top and bottom faces are not allowed to move in the  $y$  direction, and the front and back faces are not allowed to displace in the  $z$  direction. We compared the reaction forces on the left face between the two software packages. We note that reaction forces are calculated slightly differently between the two software packages. In FEBio the reaction forces are calculated at each node, while PolyFEM computes them on the surface (i.e. traction force). To convert between FEBio and PolyFEM, we needed to multiply PolyFEM's force by the cross-sectional area of the element (in this analysis we report the reaction force as defined by FEBio). We found that the two reaction forces were slightly different in value (less than 3%). This difference is likely due to differing implementations of the Mooney-Rivlin material model. However, it should be noted that the reaction force reported by PolyFEM matched the force calculated by ABAQUS.

In the next simulation, we applied a load that induced approximately 8 m of lateral deflection to a 0.15 m  $\times$  0.10 m  $\times$  10 m long rectangular cantilever beam. We meshed it with 400 hexahedral elements along its length and one through, each its width and depth. We fixed one face at the end of the length and applied a load 269.35 N to the tip at the other end, which was perpendicular to the depth of the beam. We modeled the beam using St. Venant-Kirchhoff material



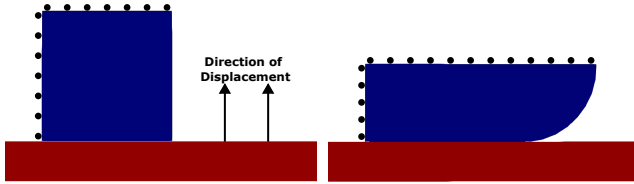
The cantilever beam in its undeformed (black vertical line) and deformed (white curve) position. The red dashed arrow shows the force of 269.35 N applied to the top face in the  $z$  direction. The force is enough to deflect the beam laterally 8 m.

**Figure 5:** Cantilever comparison between FEBio and PolyFEM.

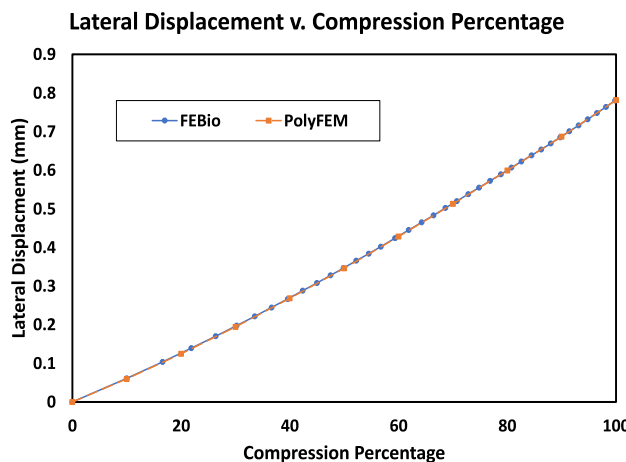
( $E = 10$  MPa,  $\nu = 0.0$ ). The beam was also fixed along its depth so that it could only deflect vertically and horizontally (Figure 5, left). The method used to apply the load at the tip differed slightly between the two solvers. In FEBio, we applied the force as a nodal force split evenly between the four nodes at the top of the beam – meaning each node was subjected to 67.3375 N of force. PolyFEM integrates the load across the surface itself, therefore we divided the applied force by the cross-sectional area (17956.66 N) in order to make the two problems equivalent. We measured the amount of lateral deflection (displacement to the left) at the center of the top face and the two solvers produced equivalent final results (Figure 5, right)

In the “upsetting of an elastic billet” simulation, we compressed to 60% of its initial height between two rigid surfaces a 1 mm  $\times$  1 mm  $\times$  0.1 mm elastic billet (meshed with  $40 \times 40 \times 1$  hexahedral elements, Figure 6, top). Using a quarter symmetry assumption, we can simulate only one-quarter of the elastic billet (Figure 6, top). This meant that the top and left sides of the billet were fixed perpendicular to those sides (modeled as rollers in Figure 6). We modeled the billet as a Mooney–Rivlin material ( $C_1 = 1$  MPa,  $C_2 = 10$  MPa,  $K = 10$  GPa). The rigid surface was modeled as an obstacle in PolyFEM and a rigid wall within FEBio. The outcome measure of this simulation is the maximum lateral displacement of the elastic billet. In this example, the solvers agreed on the lateral displacement of the top of the billet to the thousandths of a millimeter (0.781 mm, Figure 6 bottom). The simulation was significantly faster when conducted in FEBio than in PolyFEM, with a convergence time of 3 seconds and 56 seconds, respectively.

The final simulation consists of crushing a pipe ( $r_o = 114.3$  mm,  $r_i = 105.43$  mm,  $t = 25.4$  mm) by a rigid body. The pipe was modeled as a St. Venant-Kirchhoff material ( $E = 185.86$  GPa,  $\nu = 0.29972$ ) and meshed it using FEBio (Slices = 24, Segments = 4, Stacks = 1). As in the previous simulation, the rigid body was modeled as a rigid wall and obstacle in FEBio and PolyFEM, respectively. Additionally, quarter symmetry was assumed. Figure 7 shows the pipe and obstacle in the rest and deformed configurations. We were



Elastic billet at the beginning of the simulation. Black circles represent rollers as the elastic billet was constrained perpendicular to those axes.



Elastic billet Figure displacement caused by the compression of the two rigid surfaces.

**Figure 6:** Elastic billet Figure displacement caused by the compression of two rigid surfaces.

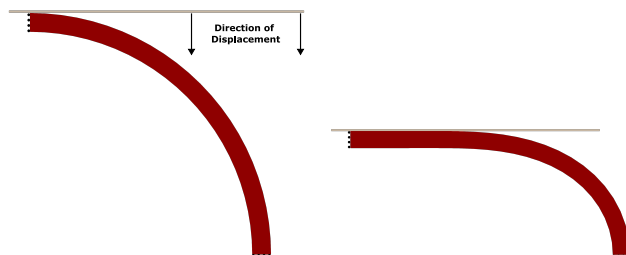


**Figure 7:** Model of a deformable pipe that was crushed between two rigid objects. The left image showed the pipe and rigid wall in the rest configuration while the image on the right showed the pipe which has been compressed to  $\approx 46\%$  its initial height

unable to directly compare the outcome measures calculated in the FEBio paper because PolyFEM does not calculate reaction forces on rigid objects. Instead, we compared the shape change between the two solvers, which were identical. Although we were unable to compare the reaction force of the rigid body we were able to show that PolyFEM is capable of correctly predicting contact-driven simulations.

We excluded five simulations from the benchmark in [38] as they contain unsupported features in PolyFEM: two tests model viscoelastic material responses, one uses shell

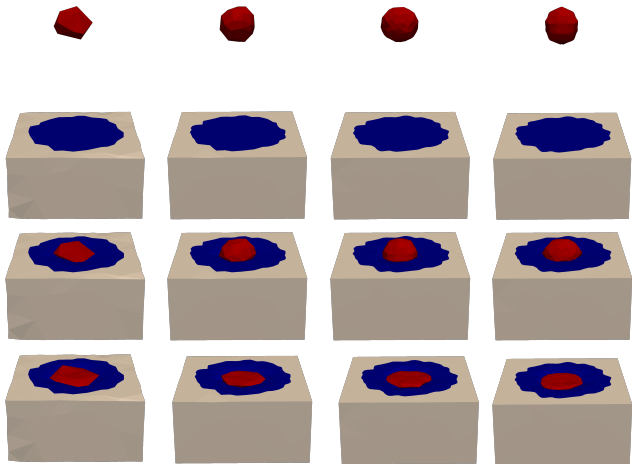


**Figure 8:** Steps of the simulation of a high energy collision between three deformable bodies (planet: red, jello: blue, and mold: off-white). Each column represents the same single simulation of the planet falling onto the jello at each of the discretization levels. For this simulation the planet and jello had moduli of 10 kPa and 100 kPa, respectively. Each row represented a different time point of the simulation. The first row shows the initial configuration of the simulation, the second shows the first contact between the planet and jello ( $t \approx 1.3$ ), and the third shows when the planet has compressed the most ( $t \approx 1.5$ ).

elements, and the final two use rigid bodies and/or shell as integral components.

#### 4.3. Planet-Fall

We developed a novel dataset to emphasize the differences between PolyFEM and FEBio, in particular in the presence of contact, large deformations, and soft materials. Every simulation in this dataset is composed of: a dodecahedron (planet) modeled as a single material, and a rectangular prism consisting of two different materials, a relatively soft “inner” material (jello), which was encased on all sides except for the top surface by a relatively stiff outer material (mold). The three materials were all modeled as NeoHookean. The bottom face of the mold was fixed in all three directions and all geometries were subject to gravity ( $9.81 \text{ ms}^{-2}$ ), which caused the planet to fall onto the top face of the jello (Figure 8).

We repeated this setup 64 times using 4 different mesh densities to mimic the normal iterative process of FE modeling and variations of moduli between the 3 materials (Table 2). We meshed the planet with 20, 203, 2002, and 20 164 tetrahedral elements while the mold and jello were meshed with a combined 1958, 3951, 8034, and 16 045 tetrahedral elements. Each discretization level was paired with the equal mesh density of the other object in the simulation (e.g., the 20 tet planet was paired with the 1958 tet mold and jello). For each discretization level, we varied the material properties of the planet and the jello between 10 kPa and 10 000 kPa; while we kept the modulus of the mold’s material constant at

**Table 2**

Runtimes of simulations in seconds. Each table corresponds to a mesh resolution; the rows and columns are the modulus of elasticity of the jello and planet, respectively. The entry in the table are of the form PolyFEM runtime (FEBio runtime); for instance, 13 (5) means that PolyFEM took 13 seconds while FEBio only 3. We use NC when the solver failed to reach a solution.

J \ P	$10^4$ Pa	$10^5$ Pa	$10^6$ Pa	$10^7$ Pa
$10^4$ Pa	69 (NC)	28 (NC)	17 (NC)	17 (NC)
$10^5$ Pa	30 (NC)	19 (4)	13 (4)	13 (5)
$10^6$ Pa	21 (NC)	17 (4)	15 (3)	11 (4)
$10^7$ Pa	20 (NC)	17 (6)	12 (3)	14 (3)
Planet (20 tet) – Jello (1958 tet)				
J \ P	$10^4$ Pa	$10^5$ Pa	$10^6$ Pa	$10^7$ Pa
$10^4$ Pa	162 (NC)	81 (NC)	57 (NC)	51 (NC)
$10^5$ Pa	108 (NC)	49 (33)	43 (15)	36 (22)
$10^6$ Pa	45 (NC)	28 (37)	24 (12)	25 (13)
$10^7$ Pa	38 (NC)	30 (NC)	24 (21)	21 (8)
Planet (203 tet) – Jello (3951 tet)				
J \ P	$10^4$ Pa	$10^5$ Pa	$10^6$ Pa	$10^7$ Pa
$10^4$ Pa	379 (NC)	212 (NC)	109 (NC)	87 (NC)
$10^5$ Pa	241 (NC)	128 (NC)	69 (204)	66 (89)
$10^6$ Pa	132 (NC)	76 (NC)	47 (NC)	43 (71)
$10^7$ Pa	124 (NC)	76 (NC)	54 (NC)	47 (70)
Planet (2002 tet) – Jello (8034 tet)				
J \ P	$10^4$ Pa	$10^5$ Pa	$10^6$ Pa	$10^7$ Pa
$10^4$ Pa	2233 (NC)	1072 (NC)	356 (NC)	220 (NC)
$10^5$ Pa	1306 (NC)	612 (NC)	283 (NC)	185 (NC)
$10^6$ Pa	689 (NC)	342 (NC)	201 (NC)	177 (NC)
$10^7$ Pa	492 (NC)	246 (NC)	178 (NC)	139 (NC)
Planet (20164 tet) – Jello (16045 tet)				

100 GPa. Similarly, we fixed the Poisson's ratio and density of all objects ( $\nu = 0.4$ ,  $\rho = 1000$ ).

We ran the simulation from a start time of 0 s to an end time of 2 s using  $dt = 0.1$  s. FEBio allows for adaptive time stepping, which we enabled to utilize the aggressive cutback option. In PolyFEM, we simply enabled contact and solved for the prescribed dt of 0.1 s. We recognize that differences in time stepping may result in different solutions; however, the goal of this set of simulations was simply to determine if the two solvers could provide solutions for these test cases since the previous sections already provided verification. In the FEBio simulation, we specified a sliding elastic contact to the planet and the top surface of the jello with the augmented Lagrangian option enabled. For each discretization level, we determined a starting value for the penalty factor by increasing the penalty factor by an order of magnitude from 1 until the planet did not pass through the jello. Then, if a simulation failed due to a negative Jacobian before completing the simulation, we adjusted the penalty by a factor of ten in both directions and retried.

We captured the runtimes (using the same computer as section 4.2) of the simulations and report them in Table 2; we

report the successful timing for all simulations that initially failed to converge in FEBio, but it is important to note that this did not include the time required to tune contact penalty appropriately and examine each simulation for penetration. This benchmark emphasizes the differences between the contact algorithms and the required human-in-loop tuning between the FE software. Overall, it was found that the simulations ran faster in FEBio for the simulations that completed in FEBio. However, it was unable to complete the entire benchmark, including the majority of the finest mesh density examples. All simulations that did not complete, failed due to the presence of negative Jacobians. Meanwhile, all of the simulations for PolyFEM completed successfully.

To provide a qualitative idea of the setup complexity, we prepared all simulations on the same computer (2017 iMac Pro, which was used to establish the runtimes). The PolyFEM simulations were prepared using the JSON file format and the FEBio simulations were prepared in FEBio Studio (version 1.8). We note that the authors were well-versed in using both of the software packages and are familiar with the process of setting up this simulation; that is, this was not a blind test. We prepared the simulations a total of five times each in alternating order (Day 1: PolyFEM, then FEBio, Day 2: FEBio, then PolyFEM, etc) on five subsequent days. We average the processing time excluding the fastest and slowest preparation time. The setup times for each of the two software packages were similar for a familiar user (219 s for PolyFEM, 214 s for FEBio). However, the biggest time save in PolyFEM (excluding the failures and subsequent parameter tuning) is when switching between the different meshes. PolyFEM only requires changing the file path to the geometry, as the boundary conditions and forces will still be applied properly. In contrast, in FEBio, the boundary conditions and body forces need to be manually recalculated and reapplied whenever the mesh changes.

#### 4.4. Hip-and-Jaw

In this experiment, we conducted biomechanical simulations of biting and pseudo-stance using PolyFEM and FEBio. To perform the simulations, we utilized patient-specific finite element (FE) models of the hip and jaw, obtained from the publicly available LibHip [43] and Open-Full-Jaw [23] repositories. The applied boundary conditions are illustrated in Figure 9. In the jaw simulation, we fixed the upper region of the maxilla mesh in all three directions, while the lower part of the mandible mesh was displaced by 0.5 mm in the positive z-direction. The mandible's side nodes were fixed in the x and y directions. In the hip simulation, we restricted the pelvic girdle by fixing the sacrum's displacement and rotation in the x, y, and z directions. We also displaced the distal ends of the two femurs by 1 mm in the positive z-direction while restricting the rest of the femur in the x and y directions. The anatomical structures in both models were assumed homogeneous and modeled as NeoHookean materials, with the teeth having  $E = 2$  GPa and  $\nu = 0.3$ , the periodontal ligament having  $E = 68.9$  MPa and  $\nu = 0.45$ , the jaw bone having  $E = 1.5$  GPa and

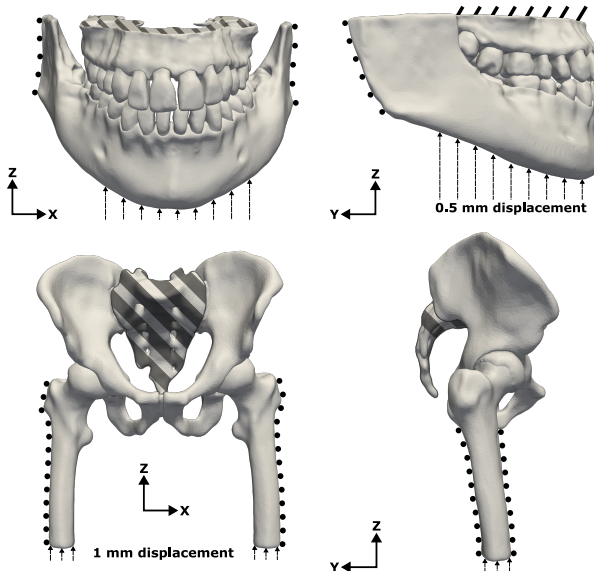


**Figure 9:** Required boundary conditions applied to the human jaw (top) and hip (bottom) to setup each simulation. Dashes represented boundaries which were fixed in all directions and rollers represented boundaries fixed perpendicular to them. In the case of the jaw simulation the upper jaw was fixed in all directions, and the lower jaw was fixed in  $x$  and  $y$  directions and displaced 0.5 mm in the positive  $z$ -direction. The sacrum was fixed in all three directions and the femurs were both fixed in the  $x$  and  $y$  directions. A displacement of 1 mm was applied to the distal end of the femur in the positive  $z$ -direction.

$\nu = 0.30$ , the hip bone having  $E = 17 \text{ GPa}$  and  $\nu = 0.30$ , and the hip cartilage having  $E = 12 \text{ MPa}$  and  $\nu = 0.45$ . For the purposes of this paper we statically simulated these simulations (solver set to static in FEBio, ignore\_inertia set to true in PolyFEM).

Due to the different contact models utilized in FEBio and PolyFEM, some simulation setups could not be replicated in both solvers. For instance, FEBio necessitated an initial penetration between contact surfaces for accurate contact detection, while PolyFEM did not require such an initial step. Therefore, to ensure simulation convergence, the distance between contact surfaces, such as the separation between two sliding cartilages in the hip joint, must be tailored to the specific solver used. If the contact model in the solver is not taken into consideration the likelihood of the simulation failing to converge raises significantly. For example, in the biting scenario, if the prescribed displacement is replaced with a pressure load, the simulation fails to converge in FEBio due to inverted elements. This issue likely arose from incorrect contact parameters, and despite our efforts to modify the applied load magnitude and adjust various contact parameters, the simulations failed in all our attempts. These findings suggest that simulations involving complex geometries, soft tissues, contacts, and complex loading conditions may require significant parameter-tuning procedures to achieve successful results. Contrarily, PolyFEM was able

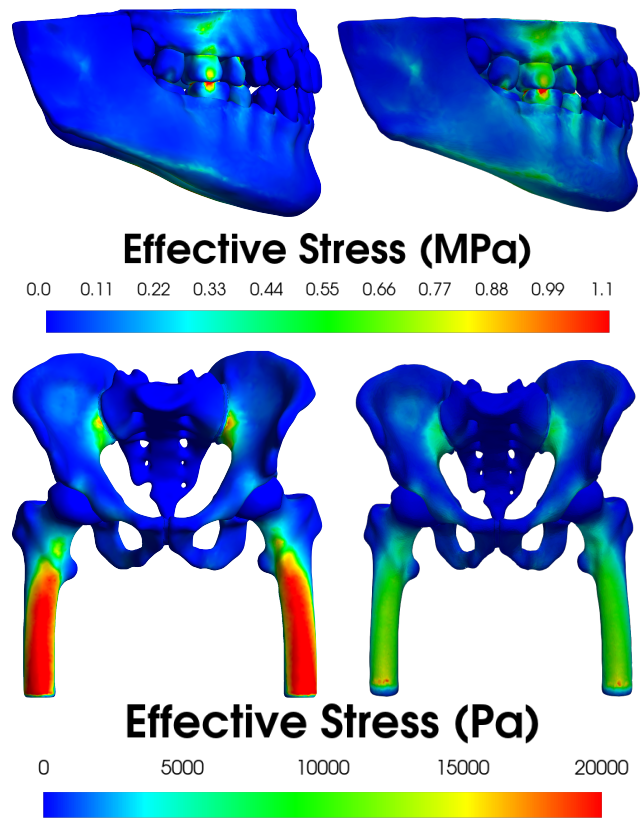


**Figure 10:** The outputs from the hip and jaw simulation from both of the FEBio (left) and PolyFEM (right). The two solvers produced very similar stress distributions across the surfaces. The only major difference was in the stress distributions in the hip simulations, this is most likely due to the differences in how the boundary conditions were applied to the models. The model created in FEBio also used rigid regions of bone to drive the displacement, which may have also contributed to differences in stress distribution.

to run the simulation with the pressure load without issues, and did not require parameter tuning.

To improve the accuracy of the simulations and avoid element-locking effects, we increased the order of the volume mesh elements. FEBio's user interface includes a tool that allows for the conversion of different element types into one another. In our case, we converted *Tet4* elements into *Tet10* elements, which resulted in an increase in the number of nodes in the jaw model by nearly 700%. However, due to the excessive memory required for such large simulation, we were unable to execute the simulations using FEBio on the same computer that was used in section 4.2 and 4.3. Using PolyFEM, we benefited the adaptive  $p$ -refinement feature, which allowed us to selectively increase the order of the basis functions used in specific domains while employing linear basis functions for the remaining domains. Using this method, we were able to perform the simulations on the same machine, and the convergence time was approximately 17 and 42 minutes in FEBio and PolyFEM, respectively. The hip simulation took significantly more time to complete in PolyFEM than FEBio (4 hours and 5 minutes, respectively).

This is likely due to the differences in contact method and methods for applying the boundary conditions. Future releases of PolyFEM will need to focus on addressing the significantly longer simulation time, however, as we have noted before there was no tuning of the models required in PolyFEM while there was a significant amount of tuning for FEBio. Additionally, we could simulate a different hip geometry without needing to change any of the boundary conditions.

## 5. Conclusions

This study demonstrated that PolyFEM produced results matching those from FEBio for previously published simulations based on solid, hyperelastic materials. This provides important verification of the solutions provided by PolyFEM. Further, this study demonstrated that PolyFEM offers solutions to problems that are challenging for other solvers such as contact or soft materials. Finally, this study demonstrated the utility of PolyFEM in solving patient-specific models in biomechanics. Thus, this alternative solver is very suitable for solving many problems in biomechanics where geometric nonlinearities are common.

It is important to note that at this stage of development, PolyFEM lacks many of the features available for other solvers. These include a user interface (PolyFEM uses a JSON setup file and Paraview for post-processing), a wide array of materials, shell and rod elements, a rigid body solver, tied-contact, a multi-physics platform, and optimization for parallel performance. However, there are plans to implement many of these features, which would help PolyFEM realize its high potential for biomechanical simulation due to its improved automation and robustness. It should also be noted that one limitation of using a barrier potential for contact is that the simulation cannot have interpenetrating surfaces in its initial configuration. This will need to be considered when creating meshes from segmented medical images. The upside of this limitation is the higher robustness and the guarantee that there will be no penetrations in all timesteps. Moreover, there are parameters that can be adjusted that can lead to improved performance for challenging simulations. At the time of writing this manuscript, those parameters have not be fully optimized, so it is anticipated that the difference in runtimes between the two solvers will improve with further development.

While PolyFEM is early in its development, it currently provides verified solutions for hyperelastic materials that are consistent with FEBio, and it is capable of simulating challenging problems in biomechanics where other solvers fail. It is also open-source and publicly available. Future work will aim to implement many of the aforementioned features to provide more options for the biomechanics community to implement it as another tool in their workflows.

## ACKNOWLEDGEMENTS

We acknowledge funding from NSF 2053851, NSF 1835712, NSF 1908767, NIH R01HD097187, NIH R01-HD083383-06, NSERC DGECR-2021-00461, RGPIN 2021-0370, Horizon2020 MSCA grant No.764644, and NIH R01DK133328.

## References

- [1] Abaqus, 2006. Abaqus Verification Manual. Verification Manual 6.6. Dassault Systems. Vélizy-Villacoublay, France.
- [2] Ammar, H.H., Ngan, P., Crout, R.J., Mucino, V.H., Mukdadi, O.M., 2011. Three-dimensional modeling and finite element analysis in treatment planning for orthodontic tooth movement. *American Journal of Orthodontics and Dentofacial Orthopedics* 139, e59–e71.
- [3] Anderson, A.E., Ellis, B.J., Weiss, J.A., 2007. Verification, validation and sensitivity studies in computational biomechanics. *Computer Methods in Biomechanics and Biomedical Engineering* 10, 171–184. doi:10.1080/10255840601160484.
- [4] Ansys, 2013. ANSYS Mechanical APDL Verification Manual. ANSYS Verification Manual 15. ANSYS inc.. Cannonsburg, PA.
- [5] Ateshian, G., Maas, S.A., Rossheron, M., 2022. FEBio software: Testsuite. <https://github.com/febiosoftware/TestSuite>.
- [6] Babuska, I., 1973. The Finite Element Method with Penalty. *Mathematics of Computation* 27, 221. doi:10.2307/2005611.
- [7] Bathe, K., 1996. *Finite Element Procedures*. 2nd ed., Prentice-Hall, Watertown, MA.
- [8] Bog, T., Zander, N., Kollmannsberger, S., Rank, E., 2015. Normal contact with high order finite elements and a fictitious contact material. *Computers & Mathematics with Applications* 70, 1370–1390. doi:10.1016/j.camwa.2015.04.020.
- [9] Burman, E., Claus, S., Hansbo, P., Larson, M.G., Massing, A., 2015. CutFEM: Discretizing geometry and partial differential equations. *International Journal for Numerical Methods in Engineering* 104, 472–501. doi:10.1002/nme.4823.
- [10] Chethan, K., Zuber, M., Shenoy, S., Kini, C.R., et al., 2019. Static structural analysis of different stem designs used in total hip arthroplasty using finite element method. *Heliyon* 5, e01767.
- [11] Claus, S., Kerfriden, P., Moshfeghifar, F., Darkner, S., Erleben, K., Wong, C., 2021. Contact modeling from images using cut finite element solvers. *Advanced Modeling and Simulation in Engineering Sciences* 8, 13. doi:10.1186/s40323-021-00197-2.
- [12] Damsgaard, M., Rasmussen, J., Christensen, S.T., Surma, E., de Zee, M., 2006. Analysis of musculoskeletal systems in the anybody modeling system. *Simulation Modelling Practice and Theory* 14, 1100–1111. doi:<https://doi.org/10.1016/j.simpat.2006.09.001>. sIMs 2004.
- [13] Dubov, A., Kim, S.Y.R., Shah, S., Schemitsch, E.H., Zdero, R., Bougherara, H., 2011. The biomechanics of plate repair of periprosthetic femur fractures near the tip of a total hip implant: the effect of cable-screw position. *Proceedings of the Institution of Mechanical Engineers, Part H: Journal of Engineering in Medicine* 225, 857–865. doi:10.1177/0954411911410642.
- [14] Elshazly, T.M., Bouraquel, C., Aldesoki, M., Ghoneima, A., Abuzayda, M., Talaat, W., Talaat, S., Keilig, L., 2022. Computer-aided finite element model for biomechanical analysis of orthodontic aligners. *Clinical Oral Investigations* 27, 115–124. doi:10.1007/s00784-022-04692-7.
- [15] Erdemir, A., Guess, T.M., Halloran, J., Tadepalli, S.C., Morrison, T.M., 2012. Considerations for reporting finite element analysis studies in biomechanics. *Journal of Biomechanics* 45, 625–633. doi:10.1016/j.jbiomech.2011.11.038.
- [16] Erdemir, A., Mulugeta, L., Ku, J.P., Drach, A., Horner, M., Morrison, T.M., Peng, G.C.Y., Vadigepalli, R., Lytton, W.W., Myers, J.G., 2020. Credible practice of modeling and simulation in healthcare: ten rules from a multidisciplinary perspective. *Journal of Translational Medicine* 18, 369. doi:10.1186/s12967-020-02540-4.

- [17] Erleben, K., 2018. Methodology for Assessing Mesh-Based Contact Point Methods. *ACM Transactions on Graphics* 37, 1–30. doi:10.1145/3096239.
- [18] Fang, G., Lin, Y., Wu, J., Cui, W., Zhang, S., Guo, L., Sang, H., Huang, W., 2020. Biomechanical Comparison of Stand-Alone and Bilateral Pedicle Screw Fixation for Oblique Lumbar Interbody Fusion Surgery—A Finite Element Analysis. *World Neurosurgery* 141, e204–e212. doi:10.1016/j.wneu.2020.05.245.
- [19] Faure, F., Duriez, C., Delingette, H., Allard, J., Gilles, B., Marchesseau, S., Talbot, H., Courtecuisse, H., Bousquet, G., Peterlik, I., Cotin, S., 2012. SOFA: A Multi-Model Framework for Interactive Physical Simulation, in: Payan, Y. (Ed.), *Soft Tissue Biomechanical Modeling for Computer Assisted Surgery*. Springer. volume 11 of *Studies in Mechanobiology, Tissue Engineering and Biomaterials*, pp. 283–321. doi:10.1007/8415\\_\\_2012\\_\\_125.
- [20] Fernandes, F.A.O., Alves de Sousa, R.J., Ptak, M., 2018. Validation of YEAHM, in: Head Injury Simulation in Road Traffic Accidents. Springer International Publishing, Cham. SpringerBriefs in Applied Sciences and Technology, pp. 41–58. doi:10.1007/978-3-319-89926-8.
- [21] Finley, S.M., Brodke, D.S., Spina, N.T., DeDen, C.A., Ellis, B.J., 2018. FEBio finite element models of the human lumbar spine. *Computer Methods in Biomechanics and Biomedical Engineering* 21, 444–452. doi:10.1080/10255842.2018.1478967.
- [22] Geng, J.P., Tan, K.B., Liu, G.R., 2001. Application of finite element analysis in implant dentistry: a review of the literature. *The Journal of prosthetic dentistry* 85, 585–598.
- [23] Gholamalizadeh, T., Moshfeghifar, F., Ferguson, Z., Schneider, T., Panozzo, D., Darkner, S., Makaremi, M., Chan, F., Søndergaard, P.L., Erleben, K., 2022. Open-Full-Jaw: An open-access dataset and pipeline for finite element models of human jaw. *Computer Methods and Programs in Biomedicine* 224, 107009. doi:10.1016/j.cmpb.2022.107009.
- [24] Guo, H., Nickel, J.C., Iwasaki, L.R., Spilker, R.L., 2012. An augmented lagrangian method for sliding contact of soft tissue. *Journal of Biomechanical Engineering*.
- [25] Guo, H., Spilker, R.L., 2011. Biphasic finite element modeling of hydrated soft tissue contact using an augmented lagrangian method. *Journal of biomechanical engineering* 133.
- [26] Henninger, H.B., Reese, S.P., Anderson, A.E., Weiss, J.A., 2010. Validation of computational models in biomechanics. Proceedings of the Institution of Mechanical Engineers, Part H: Journal of Engineering in Medicine 224, 801–812. doi:10.1243/09544119JEIM649.
- [27] Hu, P., Wu, T., Wang, H., Qi, X., Yao, J., Cheng, X., Chen, W., Zhang, Y., 2019. Biomechanical Comparison of Three Internal Fixation Techniques for Stabilizing Posterior Pelvic Ring Disruption: A 3D Finite Element Analysis. *Orthopaedic Surgery* 11, 195–203. doi:10.1111/os.12431.
- [28] Hughes, T.J., Taylor, R.L., Sackman, J.L., Curnier, A., Kanoknukulchai, W., 1976. A finite element method for a class of contact-impact problems. *Computer Methods in Applied Mechanics and Engineering* 8, 249–276. doi:10.1016/0045-7825(76)90018-9.
- [29] Humphrey, J.D., Rajagopal, K., 2002. A constrained mixture model for growth and remodeling of soft tissues. *Mathematical models and methods in applied sciences* 12, 407–430.
- [30] Jiang, T., Wu, R.Y., Wang, J.K., Wang, H.H., Tang, G.H., 2020. Clear aligners for maxillary anterior en masse retraction: a 3d finite element study. *Scientific reports* 10, 10156.
- [31] Kane, C., Marsden, J.E., Ortiz, M., West, M., 2000. Variational integrators and the newmark algorithm for conservative and dissipative mechanical systems. *Int. J. for Numer. Meth. in Eng.* 49.
- [32] Kim, Y.S., Kang, K.T., Son, J., Kwon, O.R., Choi, Y.J., Jo, S.B., Choi, Y.W., Koh, Y.G., 2015. Graft Extrusion Related to the Position of Allograft in Lateral Meniscal Allograft Transplantation: Biomechanical Comparison Between Parapatellar and Transpatellar Approaches Using Finite Element Analysis. *Arthroscopy: The Journal of Arthroscopic & Related Surgery* 31, 2380–2391.e2. doi:10.1016/j.arthro.2015.06.030.
- [33] Lew, S., Wolters, C., Dierkes, T., Röer, C., MacLeod, R., 2009. Accuracy and run-time comparison for different potential approaches and iterative solvers in finite element method based EEG source analysis. *Applied Numerical Mathematics* 59, 1970–1988. doi:10.1016/j.apnum.2009.02.006.
- [34] Li, J., 2021. Development and validation of a finite-element musculoskeletal model incorporating a deformable contact model of the hip joint during gait. *Journal of the Mechanical Behavior of Biomedical Materials* 113, 104136. doi:10.1016/j.jmbbm.2020.104136.
- [35] Li, M., Ferguson, Z., Schneider, T., Langlois, T., Zorin, D., Panozzo, D., Jiang, C., Kaufman, D.M., 2020. Incremental potential contact: intersection-and inversion-free, large-deformation dynamics. *ACM Transactions on Graphics* 39. doi:10.1145/3386569.3392425.
- [36] Logg, A., Wells, G.N., 2010. Dolfin: Automated finite element computing. *ACM Trans. Math. Softw.* 37. doi:10.1145/1731022.1731030.
- [37] Luo, J., Chen, L., Fenner, D.E., Ashton-Miller, J.A., DeLancey, J.O., 2015. A multi-compartment 3-D finite element model of rectocele and its interaction with cystocele. *Journal of Biomechanics* 48, 1580–1586. doi:10.1016/j.jbiomech.2015.02.041.
- [38] Maas, S.A., Ellis, B.J., Ateshian, G.A., Weiss, J.A., 2012. FEBio: Finite elements for biomechanics. *J Biomech Eng* 134.
- [39] Mazier, A., Bilger, A., Forte, A.E., Peterlik, I., Hale, J.S., Bordas, S.P.A., 2022. Inverse deformation analysis: an experimental and numerical assessment using the fenics project. *Engineering with Computers* 38, 4099–4113. doi:10.1007/s00366-021-01597-z.
- [40] Ménager, E., Schegg, P., Khairallah, E., Marchal, D., Dequidt, J., Preux, P., Duriez, C., 2022. SofaGym: An open platform for Reinforcement Learning based on Soft Robot simulations. *Soft Robotics*.
- [41] Meng, Q., Jin, Z., Fisher, J., Wilcox, R., 2013. Comparison between FEBio and Abaqus for biphasic contact problems. *Proceedings of the Institution of Mechanical Engineers. Part H, Journal of engineering in medicine* 227, 1009–1019. doi:10.1177/0954411913483537.
- [42] Mengoni, M., 2021. Biomechanical modelling of the facet joints: a review of methods and validation processes in finite element analysis. *Biomechanics and Modeling in Mechanobiology* 20, 389–401. doi:10.1007/s10237-020-01403-7.
- [43] Moshfeghifar, F., Gholamalizadeh, T., Ferguson, Z., Schneider, T., Nielsen, M.B., Panozzo, D., Darkner, S., Erleben, K., 2022. LibHip: An open-access hip joint model repository suitable for finite element method simulation. *Computer Methods and Programs in Biomedicine* 226, 107140. doi:10.1016/j.cmpb.2022.107140.
- [44] Nocedal, J., Wright, S.J., 2006. Penalty and Augmented Lagrangian Methods, in: *Numerical Optimization*. Springer New York, New York, NY, pp. 497–528. doi:10.1007/978-0-387-40065-5\_17.
- [45] Oefner, C., Herrmann, S., Kebbach, M., Lange, H.E., Kluess, D., Woiczinski, M., 2021. Reporting checklist for verification and validation of finite element analysis in orthopedic and trauma biomechanics. *Medical Engineering & Physics* 92, 25–32. doi:10.1016/j.medengphy.2021.03.011.
- [46] Peng, M.J.Q., Xu, H., Chen, H.Y., Lin, Z., Li, X., Shen, C., Lau, Y., He, E., Guo, Y., 2020. Biomechanical analysis for five fixation techniques of Pauwels-III fracture by finite element modeling. *Computer Methods and Programs in Biomedicine* 193, 105491. doi:10.1016/j.cmpb.2020.105491.
- [47] Pirmoradian, M., Naeeni, H.A., Firouzbakht, M., Toghraie, D., Darabi, R., et al., 2020. Finite element analysis and experimental evaluation on stress distribution and sensitivity of dental implants to assess optimum length and thread pitch. *Computer methods and Programs in Biomedicine* 187, 105258.
- [48] Puso, M.A., Laursen, T.A., 2004. A mortar segment-to-segment contact method for large deformation solid mechanics. *Computer Methods in Applied Mechanics and Engineering* 193, 601–629. doi:10.1016/j.cma.2003.10.010.
- [49] Ratajczak, M., Ptak, M., Chybowski, L., Gawdzińska, K., Będziński, R., 2019. Material and Structural Modeling Aspects of Brain Tissue Deformation under Dynamic Loads. *Materials* 12, 271. doi:10.3390/

- ma12020271.
- [50] Routzong, M.R., Martin, L.C., Rostaminia, G., Abramowitch, S., 2021. Urethral support in female urinary continence part 2: a computational, biomechanical analysis of Valsalva. International Urogynecology Journal doi:10.1007/s00192-021-04694-1. publisher: International Urogynecology Journal.
  - [51] Routzong, M.R., Moalli, P.A., Maiti, S., De Vita, R., Abramowitch, S.D., 2019. Novel simulations to determine the impact of superficial perineal structures on vaginal delivery. Interface Focus 9, 20190011. doi:10.1098/rsfs.2019.0011.
  - [52] Schneider, T., Dumas, J., Gao, X., Zorin, D., Panozzo, D., 2019. Polyfem. <https://polyfem.github.io/>.
  - [53] Seth, A., Hicks, J.L., Uchida, T.K., Habib, A., Dembia, C.L., Dunne, J.J., Ong, C.F., DeMers, M.S., Rajagopal, A., Millard, M., Hamner, S.R., Arnold, E.M., Yong, J.R., Lakshmikanth, S.K., Sherman, M.A., Ku, J.P., Delp, S.L., 2018. Opensim: Simulating musculoskeletal dynamics and neuromuscular control to study human and animal movement. PLOS Computational Biology 14, 1–20. doi:10.1371/journal.pcbi.1006223.
  - [54] Shu, L., Li, S., Sugita, N., 2020. Systematic review of computational modelling for biomechanics analysis of total knee replacement. Bio-surface and Biotribology 6, 3–11.
  - [55] Simo, J.C., Wriggers, P., Taylor, R.L., 1985. A perturbed Lagrangian formulation for the finite element solution of contact problems. Computer Methods in Applied Mechanics and Engineering 50, 163–180. doi:10.1016/0045-7825(85)90088-X.
  - [56] Song, M., Sun, K., Li, Z., Zong, J., Tian, X., Ma, K., Wang, S., 2021. Stress distribution of different lumbar posterior pedicle screw insertion techniques: a combination study of finite element analysis and biomechanical test. Scientific Reports 11, 129–68. doi:10.1038/s41598-021-90686-6.
  - [57] Takhounts, E., Eppinger, R., Campbell, J.Q., Rabih, T., Power, E., Shook, L., 2003. On the Development of the SIMon Finite Element Head Model. Stapp Car Crash Journal 2003, 107–33.
  - [58] Takhounts, E.G., Ridella, S.A., Hasija, V., Tannous, R.E., Campbell, J.Q., Malone, D., Danelson, K., Stitzel, J., Rowson, S., Duma, S., 2008. Investigation of traumatic brain injuries using the next generation of simulated injury monitor (SIMon) finite element head model. Stapp Car Crash Journal 52. doi:10.4271/2008-22-0001.
  - [59] Taylor, R.L., 1980. Contact-impact Problems: Engineering report and user's manual. volume 1. The Administration.
  - [60] Van Staden, R., Guan, H., Loo, Y.C., 2006. Application of the finite element method in dental implant research. Computer methods in biomechanics and biomedical engineering 9, 257–270.
  - [61] Wang, B., Ferguson, Z., Schneider, T., Jiang, X., Attene, M., Panozzo, D., 2021. A large scale benchmark and an inclusion-based algorithm for continuous collision detection. ACM Trans. Graphic. 40.
  - [62] Wriggers, P., 1995. Finite element algorithms for contact problems. Archives of Computational Methods in Engineering 2, 1–49. doi:10.1007/BF02736195.
  - [63] Wriggers, P., Zavarise, G., 2007. A formulation for frictionless contact problems using a weak form introduced by Nitsche. Computational Mechanics 41, 407–420. doi:10.1007/s00466-007-0196-4.
  - [64] Zavarise, G., De Lorenzis, L., 2009. The node-to-segment algorithm for 2D frictionless contact: Classical formulation and special cases. Computer Methods in Applied Mechanics and Engineering 198, 3428–3451. doi:10.1016/j.cma.2009.06.022.
  - [65] Zeng, Z., Cotin, S., Courtecuisse, H., 2022. Real-Time FE Simulation for Large-Scale Problems Using Precondition-Based Contact Resolution and Isolated DOFs Constraints. Computer Graphics Forum 41, 418–434. doi:10.1111/cgf.14563.
  - [66] Zhang, K., Li, L., Yang, L., Shi, J., Zhu, L., Liang, H., Wang, X., Yang, X., Jiang, Q., 2019. The biomechanical changes of load distribution with longitudinal tears of meniscal horns on knee joint: a finite element analysis. Journal of Orthopaedic Surgery and Research 14, 237. doi:10.1186/s13018-019-1255-1.
  - [67] Zhou, Z., Li, X., Kleiven, S., Shah, C.S., Hardy, W.N., 2018. A Reanalysis of Experimental Brain Strain Data: Implication for Finite Element Head Model Validation. Stapp Car Crash Journal 62, 293–318. doi:10.4271/2018-22-0007.
  - [68] Zimmerman, B.K., Ateshian, G.A., 2018. A Surface-to-Surface Finite Element Algorithm for Large Deformation Frictional Contact in febio. Journal of Biomechanical Engineering 140. URL: <https://doi.org/10.1115/1.4040497>, doi:10.1115/1.4040497, arXiv:<https://asmedigitalcollection.asme.org/biomechanical/article-pdf/140/8/081013>.
  - [69] Zupancic Cepic, L., Frank, M., Reisinger, A., Pahr, D., Zechner, W., Schedle, A., 2022. Biomechanical finite element analysis of short-implant-supported, 3-unit, fixed CAD/CAM prostheses in the posterior mandible. International Journal of Implant Dentistry 8, 8. doi:10.1186/s40729-022-00404-8.



**Declaration of interests**

The authors declare that they have no known competing financial interests or personal relationships that could have appeared to influence the work reported in this paper.

The authors declare the following financial interests/personal relationships which may be considered as potential competing interests: